American Journal of Pathology, Vol. 158, No. 4, April 2001

Chemokine Expression Dynamics in Mycobacterial (Type-1) and Schistosomal (Type-2) Antigen-Elicited Pulmonary Granuloma Formation

Boqin Qiu,* Kirsten A. Frait,† Filip Reich,† Eric Komuniecki,† and Stephen W. Chensue*†

From the Departments of Pathology and Laboratory Medicine,† Veterans Affairs Medical Center, Ann Arbor; and the Department of Pathology, University of Michigan Hospitals, Ann Arbor, Michigan*

Transcript expression of 24 chemokines (CKs) was examined throughout 8 days in mouse lungs with type-1 (Th1) or type-2 (Th2) cytokine-mediated granulomas induced by bead-immobilized mycobacterial purified protein derivative or *Schistosoma mansoni* egg antigens. Where possible, CK protein levels were also measured. In addition, we examined effects of *in vivo* cytokine depletions. Findings were as follows: 1) bead challenge induced increases in 18 of 24 CK transcripts with type-1 and type-2 responses displaying different patterns. CKs fell into four categories: a) type-1-dominant (γ-interferon-inducible protein (IP-10), monokine induced by INF-γ (MIG), macrophage inflammatory protein-2 (MIP-2), lipopolysaccharide-induced chemokine (LIX), rodent growth-related oncogene homologue (KP), macrophage inflammatory protein-1α (MIP-1α) and -1β (MIP-1β), lymphotactin), b) type-2-dominant (eotaxin, monocyte chemotactic protein-2 (MCP-2) and -3 (MCP-3), liver and activation-regulated chemokine (LARC), T cell activation protein-3 (TCA-3), c) type-1 and type-2 co-dominant (MCP-1, MCP-5, monocyte-derived chemokine (MDC), thymus and activation-related chemokine (TARC), C10), and d) constitutive (lungkine, secondary lymphoid-tissue chemokine (SLC), EBI1-ligand chemokine (ELC), fractalkine, macrophage inflammatory protein-1γ (MIP1-γ), and stromal cell derived factor-1α (SDF1-α). 2) CKs displayed characteristic temporal patterns. CXC (IP-10, MIG, MIP-2, LIX, KC) and certain CC (MCP-1, MCP-5, MIP-1α, MIP-1β) CKs were produced maximally within 1 to 2 days. Others (MCP-2, MCP-3, eotaxin, lymphotactin, LARC, TCA-3) displayed peak expression later. 3) Interferon-γ neutralization profoundly abrogated MIG, but had little effect on other CKs. Tumor necrosis factor-α neutralization caused up to 50% reduction in a range of CKs. These findings indicate that type-1 and type-2 granulomas display characteristic CK profiles with coordinated expression that is under cytokine-mediated regulation. ***(Am J Pathol 2001, 158:1503–1515)***

A boggling array of chemokines (CKs) has been described and detected at local inflammatory sites.[1] *In vitro* studies indicate that they are produced to different degrees by a wide variety of cell types in response to injury, endogenous mediators, and exogenous stimulants. However, the *in vivo* organization and regulation of CKs is primarily unknown. It is a widely accepted hypothesis that tissue inflammation is the result of leukocytes interacting with cytokines and CKs. Each of these elements changes constantly with time. Therefore, a comprehensive, systematic approach is needed for analysis. In the present study we applied such an approach using defined, polarized models of T-cell-mediated type-1 and type-2 pulmonary granuloma formation to test the hypothesis that inflammatory responses can be defined based on profiles of CK expression.

Granulomas represent a sequestration response elicited by a remarkably diverse group of agents. They are formed by an influx of inflammatory leukocytes that aggregate often in association with a poorly digestible nidus and include mononuclear phagocytes as a defining component. In immunologically active granulomas, additional cells, such as lymphocytes and in some instances plasma cells, myofibroblasts, B cells, and eosinophils may also be recruited. Granuloma macrophages and lymphocytes are heterogeneous and change constantly throughout time with each producing a myriad of secretory products.[2,3] CKs are beginning to be recognized as one important group of mediators of granuloma formation.[4]

The present study monitored the expression of 24 CKs throughout an 8-day study period in lungs with granulomas induced by agarose bead-immobilized *Mycobacteria bovis* purified protein derivative (PPD) or *Schistosoma*

Supported by the Department of Veterans Affairs and National Institutes of Health–National Institute of Allergy and Infectious Diseases grant AI43460. B. Q. is supported by HL07517 training grant (T32).

Accepted for publication January 5, 2001.

Address reprint requests to Stephen W. Chensue, M.D., Ph.D., Pathology and Laboratory Medicine 113, Veterans Affairs Medical Center, 2215 Fuller Rd., Ann Arbor, MI 48105. E-mail: schensue@umich.edu.

mansoni egg antigens (SEA).[5] Granulomas induced by PPD-coated beads are driven primarily by the Th1 (type-1)-associated cytokines interferon (IFN)-γ and tumor necrosis factor (TNF)-α, whereas those induced by SEA-coated beads are mediated by the Th2 (type-2)-associated cytokines, IL-4 and IL-13.[6] Transcript analysis of 24 CKs in these models indicated that 18 were induced and expression showed close association with granuloma development. Moreover, among these, 13 showed type-specific and temporal differences in their expression patterns. In addition, the role of cytokine-mediated regulation was tested by intraperitoneal injection of antibodies against IFN-γ or TNF-α. MIG expression was dramatically reduced by the neutralization of IFN-γ, whereas other CKs showed no significant changes. In contrast, TNF-α neutralization reduced a broad range of CKs. This study emphasizes the importance of a comprehensive approach to CK analysis and indicates that CK profiling may be a feasible approach to define inflammatory responses for CK targeted therapies.

Materials and Methods

Animals

Female CBA/J mice were purchased from The Jackson Laboratory (Bar Harbor, ME). All mice were maintained under specific pathogen-free conditions and used at 7 to 8 weeks of age.

Sensitization and Granuloma Induction

Types 1 and 2, secondary Ag-bead granulomas were generated as previously described.[5] Briefly, mice were sensitized by a subcutaneous injection of 20 μg of *Mycobacteria bovis* purified protein derivative (PPD) (Department of Agriculture, Veterinary Division, Ames, IA) incorporated into 0.25 ml of complete Freund's adjuvant (CFA) (Sigma, St. Louis, MO) or 3,000 *Schistosoma mansoni* eggs suspended in 0.5 ml of phosphate-buffered saline (PBS). Fourteen to 16 days later, PPD- and schistosome egg-sensitized mice were respectively challenged by tail vein injections with 6,000 Sepharose 4B beads (in 0.5 ml of PBS) covalently coupled to PPD or to soluble schistosome egg antigens (SEA) obtained from the World Health Organization (Geneva, Switzerland).

Granuloma Dispersal and Morphometric Analysis

Groups of mice were killed at 1, 2, 4, and 8 days of granuloma formation. After perfusion with cold RPMI, lungs excluding trachea and major bronchi were excised. The right upper lung of each mouse was used for mRNA isolation. The left lower lobe was postinflated and formalin-fixed for granuloma size determination. The remaining lung was placed in cold RPMI medium then granulomas were isolated and dispersed as previously described.[6] For differential counting, duplicate cytospin preparations were prepared from the remaining dispersed granuloma cells and stained with Wright's stain.

Granulomas were measured blindly from formalin-inflated lungs that were paraffin-embedded, sectioned, then stained with hematoxylin and eosin. Granuloma area was measured by computerized morphometry. Only granulomas sectioned through the central bead nidus were measured. A minimum of 20 lesions was measured per lung. The total number of cells in a granuloma cross-section was determined morphometrically by directly counting cell number in an area of 2.5×10^3 μm^2. This was determined to be 32 ± 7 with each cell occupying an average of 80 ± 18 μm^2. The proportion of cell types was calculated by multiplying the total cell number by the percentages obtained by direct differential analysis of dispersed granulomas.

In Vivo *Cytokine Depletion*

At the time of bead challenge, mice were given an intraperitoneal injection of 5 mg of rabbit IgG with specificity for murine IFN-γ or TNF-α prepared by protein A column purification. Nonimmune rabbit IgG served as a control. The specificity and potency of these preparations was previously reported.[5] Two days after challenge, lungs were excised for mRNA measurement and morphometric analysis.

Preparation of mRNA and Protein Extracts from Lungs

Mice were anesthetized and bled before sacrifice for lung harvest, which was done at 1, 2, 4, and 8 days after the bead embolization. Unchallenged mice at 14 days after sensitization served as time 0 controls, whereas lungs of normal mice provided baseline determinations. After perfusion with cold RPMI, lungs, excluding the trachea and major bronchi, were excised. The left lower lung lobe of each mouse was postinflated and formalin-fixed. The right lobe was snap-frozen in liquid nitrogen for mRNA isolation, and the remaining lobes were uses for protein extraction. mRNA was isolated from the frozen tissues using Poly(A)Pure mRNA isolation kits (Ambion, Austin, TX). For protein extraction, frozen lungs were placed into Dulbecco's modified Eagle's medium and were ground using a homogenizer. Samples were centrifuged and supernatant fluids collected.

Chemokine Primers and Probes

Primers and probes were designed with primer design software (Primer Premier; Biosoft International, Palo Alto, CA) using murine sequences obtained from the National Center for Biotechnology Information (NCBI) GenBank. Table 1 shows the sequences and NCBI reference numbers. Oligonucleotides were obtained from Operon Technologies, Inc., Alameda, CA.

Table 1. Chemokine Probe and Primer Sequences

Chemokine	NCBI accession No.	Probe (5′-3′)	Sense primer (5′-3′)	Antisense primer (5′-3′)
LIX	MMU27267	TGA GGA CTC TGA CCC CAG TGA A	AAT GCA CTC GCA GTG GAA AG	ACT TGT GAG ATG AGC AGG AAG C
MIG	M34815	GGC CTG TCT GTT TGC TGG TGA G	GGG CAA GTG TCC CTT TCC TTC	GGG CTC TAG GCT GAC CCA AAT
IP-10	MUSIP10	CTC ATC CTG CTG GGT CTG AGT GG	CA TCA GCA CCA TGA ACC CAA G	CT ATG GCC CTC ATT CTC ACT G
MIP-2	MMMIP2	GCT GTC CCT CAA CGG AAG AAC C	CAA GGC TAA CTG ACC TGG AAA G	CAT AAC AAC ATC TGG GCA ATG
KC	J04596	AGC GCT GCT GCT GCT GGC	CCA GCC ACC CGC TCG CTT	GGG CCC TGA GGG CAA CAC
MIP-1α	MUSMIP1A	TTG AGC CGA ACA TTC CTG CCA CC	ATC ACT GAC CTG GAA CTG AAT G	CAA GTG AAG AGT CCC TCG ATG
MIP-1β	MUSMIP1X	GGC TCT GAC CCT CCC ACT TCC TG	AC CAT GAA GCT CTG CGT GTC	AA GCT GCC GGG AGG TGT AAG
MCP-1	MUSGFJE	CTG CAT CTG CCC TAA GGT CTT CA	TGC TGA CCC CAA GAA GGA ATG	C TTG AGG TGG TTG TGG AAA AGG
MCP-2	AB023418	TAC ATG GAG ATC CTT GAC CAG A	CTT CGG GTG CTG AAA AGC TAC	TG CCT GGA GAA GAT TAG GGG AG
MCP-3	S71251	TTC CTC ACC GCT GTT CTT TCT G	GTG CCT GAA CAG AAA CCA ACC T	CAT TCC TTA GGC GTG ACC ATT
MCP-5	MMU50712	CAC AAG CAG CCA GTG TCC CCG	AGG TAT TGG CTG GAC CAG ATG	TTC TCC TTG GGG TCA GCA CAG
Lymphotactin	MMU15607	AGG AGC CCA GAG GTC CAC CAG CA	CAG GGC CAG TAC CAG AAA GAA CA	TG GGT TTG GGA ACT GAG ATG AGC
Eotaxin	U26426	CTC CAT CCC AAC TTC CTG CTG	TTC TAT TCC TGC TGC TCA CGG	AGG GTG CAT CTG TTG TTG GTG
TCA-3	MMTCA3G	CCC TGC TAA CCG GGG TGA AGA TG	AAA GAT GGG CTC CTC CTG TCC	TGG AGG ACT GAG GGA AAC TGC
LARC	AB015136	AAG CAG AAC TGG GTG AAA AGG	GCA GCA AGC AAC TAC GAC TG	CTC TTA GGC TGA GGA GGT TC
MDC	AF052505	GGA GGA CCT GAT GAC CAT GGG TC	AGG CAG GTC TGG GTG AAG AAG CT	GG ATG GAG GTG AGT AAA GGT GGC
C10	MUSC10	TTT AGA GCA GTC AAC AGT ATT CA	CA CCC ACT TTC TTC TGT CTT CC	TA CAA CTC CAG ATG GCT CTA ACC
TARC	MMU242587	AGG CCG TGA CCT TCC CGC TGA	CAG GGA TGC CAT CGT GTT TCT	GGT CAC AGG CCG CTT TAT GTT
Lungkine	AF082859	CCC CTT TAT TGA CTG ACA AAC TA	TAT TCC CGC GTT AGT CTG GTG	G CCC ATA GTG GAG TGG GAT AAG
SLC	AF001980	TCT AAG CCT GAG CTA TGT GCA A	ATC CCG GCA ATC CTG TTC TCA CC	GC CCT TGG AGC CCT TTC CTT TC
ELC	AF059208	CCC CTG TGA ACC CGT CGG AGC CT	AGG ACA TCT GAG CGA TTC CAG	AG TCT TCC GCA TCA TTA GCA C
Fractalkine	AF071549	TGT GCT GAC CCG AAG GAG AAA TG	CT CAT CCG CTA TCA GCT AAA C	TTG TCC ACC CGC TTC TCA AAC
MIP-1γ	MMU49513	CTC CTT CCT CAT TCT TAC AAC TG	TGC CCA CTA AGA AGA TGA AGC	CAA TTT CAA GCC CTT GCT GTG
SDF-1α	MUSSDF1A	TCG ACA GAT GCC TTG TCC TGA GT	GAG AAA CCT TCC ACC AGA GCA G	GG CAC TGA ACT GGA TAA AGG AGC
Cyclophilin	MUSCYCLOA	CAT CGT GTC ATC AAG GAC TTC A	GTG GGC TCC GTC GTC TTC CTT T	C TTT CCT CCT GTG CCA TCT CCC

Polymerase Chain Reaction (PCR)-Enzyme-Linked Immunosorbent Assay (ELISA) Chemokine mRNA Detection

Reverse Transcription of the mRNA Samples

Approximately, 1 μg of mRNA was reverse-transcribed in a 20-μl reaction in a PCR reaction tube using Reverse Transcription System kits (Promega, Madison, WI). Five to 10 reactions were conducted on the same mRNA preparation in parallel to minimize variability. The cDNA product from each tube was pooled for analysis.

Equalization of the cDNA Concentrations

The concentration of each cDNA sample was adjusted so that the signal obtained with the housekeeping gene, cyclophilin, when amplified by a 22-cycle PCR reaction and detected by a PCR-ELISA, would give an absorbance value at ~0.5.

Optimization of PCR Cycle Number for each Chemokine Primer and Probe Set

After adjusting the cDNA concentration, a sample of cDNA from normal lungs was amplified by a PCR reaction using primer pairs specific for a given CK. A series of PCR reactions was performed at different cycle numbers, then the PCR products were detected by using PCR-ELISA detection kits (Roche Molecular Biochemicals, Mannheim, Germany). The cycle number giving an absorbance value nearest 0.2 was used for that particular CK primer-probe set. This was done for each of the CKs examined.

PCR-ELISA Detection of Chemokine mRNA

Each CK cDNA was amplified in a 40-μl PCR reaction, then 20 μl of the product was assayed using a biotinylated probe and PCR-ELISA (DIG Detection) kits (Roche Molecular Biochemicals). In each PCR-ELISA detection assay, PCR products were detected in duplicates. Water was used as negative control. Cyclophilin mRNA of each sample, amplified in a separate tube, was included for normalization and confirmation of cDNA equivalency. To validate the calibration curve (see below) for a particular assay, a selected preparation was assayed at both 10- and 40-μl volume, which should result in a one to four relationship in relative concentration. The basis for the quantification of mRNA expression is that the absorbance [optical density (OD^{450})] reading increases directly with the copy number of the CK mRNA being measured at the optimal PCR cycle number. However, the relationship between the OD reading and the copy number may not be linear at high OD^{450} readings. The system was therefore calibrated to correct for possible nonlinear relationships because of high copy number expression. Standard curves were generated using serially diluted cDNA samples from normal lung amplified with cyclophilin primers. The resulting curve was best fitted to obtain the following correction formulas: 1) for $OD^{450} > 1.0$: log (dilution factor) = log (OD^{450} /0.2)/0.7 and 2) for $OD^{450} < 1.0$: log (dilution factor) = ($0.9/OD^{450}(OD^{450} - 0.1)$. The formulas give the relationship between the OD^{450} reading and the relative concentration (dilution factor) of the mRNA. Using the formulas, the relative concentration of a CK mRNA in a sample was calculated from its OD^{450} reading measured from a PCR-ELISA assay.

Data Presentation

Samples of cDNA were usually run in groups of 10 or more representing a complete time course and controls. Because the results represent relative measures, they are expressed as arbitrary units defined as follows: specifically, the highest calculated mRNA expression of a particular target gene among a full set of samples was set at 100 units with levels of others adjusted against it accord-

ingly. This approach did not affect the relationship between samples and allowed for good interexperimental reproducibility.

Chemokine Protein Measurement

Snap-frozen lung lobes were suspended in 2 ml of PBS and homogenized for 20 seconds using a Tissue Tearor (Biospec Products, Inc., Bartlesville, OK). Next, 0.1 ml of fetal bovine serum was added as a protein stabilizer. The homogenate was centrifuged at 3,000 × *g* for 20 minutes and then the supernate was collected, aliquoted, and frozen at −80°C before cytokine assay. CK protein (MIG, IP-10, KC, MIP-1α, MIP-1β, MCP-1, MDC, eotaxin, and C10) was measured in the whole lung aqueous extracts by specific ELISA using commercial reagents (R&D Systems, Minneapolis, MN, and Pharmingen, La Jolla, CA). Next, total lung protein concentration was determined in experimental and control samples, then CK levels were normalized to mg lung protein after subtraction of the fetal bovine serum protein component.

Statistics

The paired Student's *t*-test was used to compare paired groups. Values of $P > 0.05$ were considered to indicate lack of significance.

Results

Kinetics of Granuloma Growth and Leukocyte Recruitment

The kinetics of type-1 (PPD) and type-2 (SEA) bead granuloma formation are shown in Figure 1 along with leukocyte differential analyses indicating the numbers of each major cell type present in an average granuloma cross-section. It can be seen that the period of rapid cellular accumulation occurred between 0 and 4 days. Day 4 represented a time of lesion sustenance whereas day 8 marked the period of lesion involution. Although both type-1 and type-2 lesions contained significant components of lymphocytes by day 2, the type-1 lesion was characterized by recruitment of greater numbers of neutrophils in this period. Thereafter, on days 4 and 8, the type-2 lesion was distinguished by a significant component of eosinophils. In both types of lesions mononuclear phagocytes reached a maximum on day 4. This analysis provided a base of histopathological observations to which CK expression dynamics could be related.

Chemokine mRNA Expression Profiles during Type-1 (PPD) and Type-2 (SEA) Pulmonary Granuloma Formation

The expression profiles of 24 CK transcripts were determined for type-1 and type-2 granulomas throughout an 8-day study period. Samples from 5-day points for each

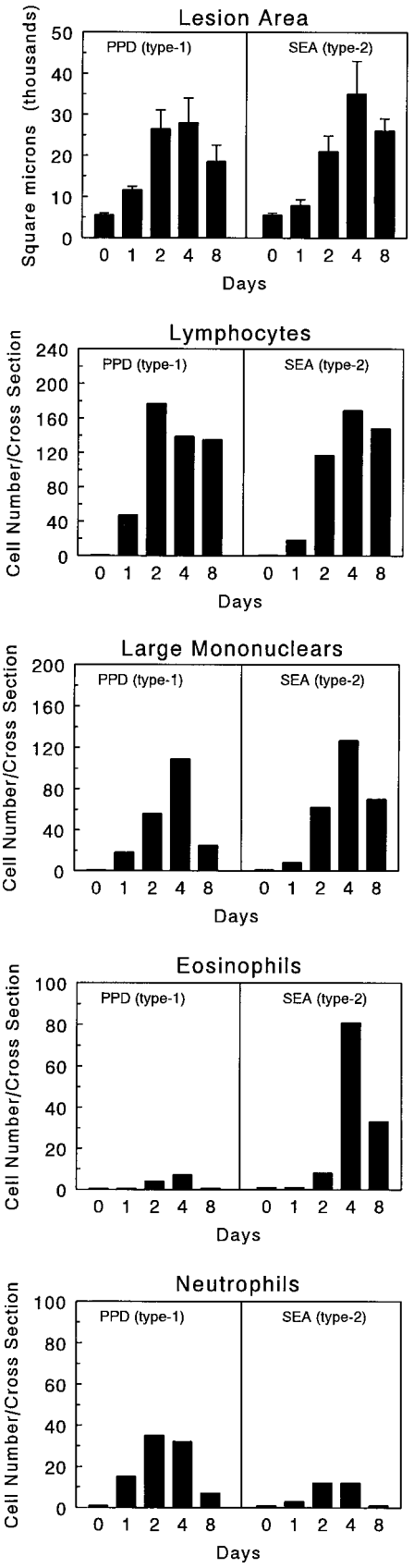

Figure 1. Kinetics of lesion growth and cell recruitment during type-1 (PPD) and type-2 (SEA) Ag-bead lung granuloma formation. Granuloma sizes and compositions were determined throughout 8 days as described in Materials and Methods. Bars were derived from analysis of six mice.

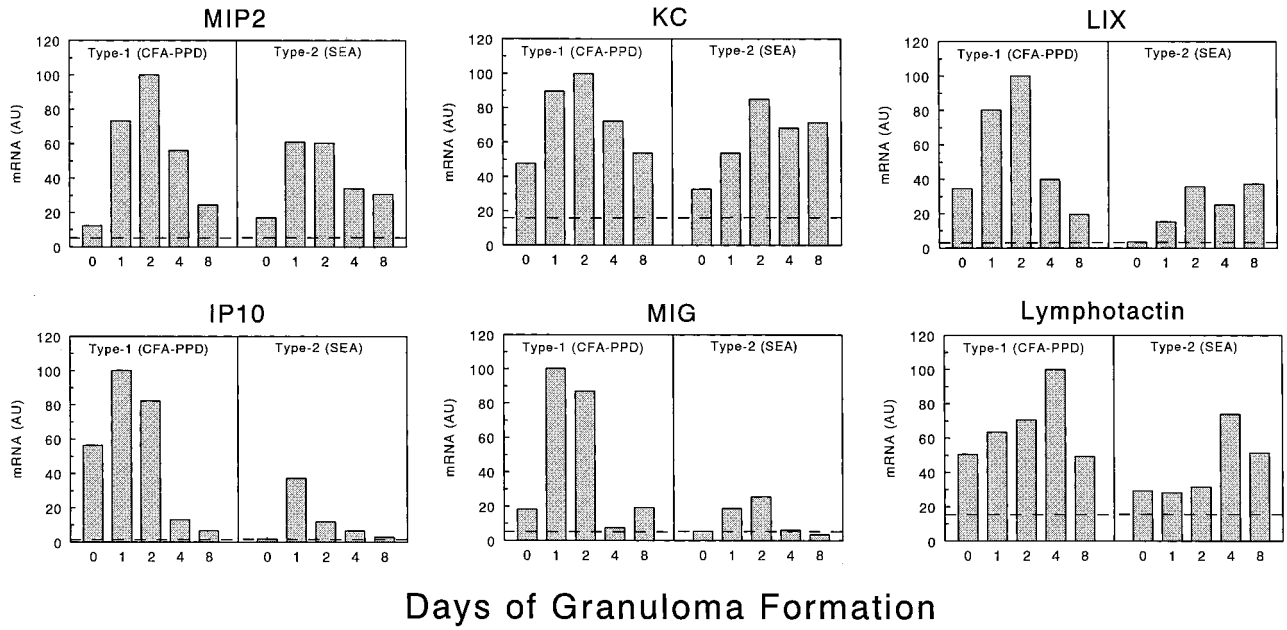

Figure 2. CXC and C chemokine mRNA expression profiles of lungs during type-1 (PPD) and type-2 (SEA) Ag-bead lung granuloma formation. The mRNA expression levels were determined by PCR-ELISA analysis and the results are presented in arbitrary units (AU) as described in Materials and Methods. The profiles are representative of at least three independent experiments. In each experiment mRNA was prepared from three to four mice for each time point. **Dashed lines** indicate levels in normal lung controls.

of the two models were measured in a single PCR-ELISA experiment and the relative abundance of each chemokine RNA was compared between the samples. Three repetitions were performed for each chemokine in three separate experiments, and only one experiment is presented. As is required for all relative RNA quantification methods, compared samples were measured together in each experiment. Although results could not be pooled among experiments, the relationships were consistent within the three studies. Of the 24, 18 CKs showed significant up-regulation (greater than twofold) during granuloma development. These are presented in Figures 2 and 3. Figure 2 shows the profiles of three ELR+ CXC CKs (MIP-2, KC, and LIX), two ELR- CXC CKs (IP-10 and MIG), and one known C class CK (lymphotactin). The differences between the type-1 and type-2 granulomas were easily seen. Of these, all but KC showed a predominant expression in the type-1 response. Moreover, in the complete Freund's adjuvant-PPD sensitized mice, transcript levels for several of these (KC, LIX, IP-10, and lymphotactin) were significantly elevated before bead challenge (time 0) as compared to lungs of unsensitized, unchallenged mice (dashed line). In addition, other than lymphotactin, which reached maximum expression on day 4, the others displayed maximal expression during the rapid recruitment stage, days 1 and 2.

Figure 3 shows the profiles obtained for 12 selected CC CKs, MIP-1α, MIP-1β, MCP-1, MCP-2, MCP-3, MCP-5, TCA-3, eotaxin, LARC, TARC, C10, and MDC. Among these, MIP-1α and MIP-1β appeared to be more strongly expressed in the type-1 lesions especially on day 2. In contrast, MCP-2, MCP-3, TCA-3, eotaxin, and LARC tended to greater expression or were sustained longer in the type-2 response, especially during the later stages of granuloma formation, days 4 and 8. It was also noted that baseline levels of eotaxin transcripts were increased in lungs after sensitization (compare day 0 to dashed line). Others such as MCP-1, MCP-5, MDC, and TARC were significantly induced in both responses, but despite trends, definite patterns of dominance could not be established. However, MCP-5 transcripts did show a unique pattern appearing to dominate early in the type-2 but later in the type-1 response.

Among the 24 CK transcripts analyzed, six were found to be expressed constitutively by lung tissue and showed no change, minimal induction, or partial inhibition after sensitization and challenge. These included ELC, fractalkine, lungkine, SLC, SDF-1α, and MIP-1γ (Figure 4). It is noteworthy that among these, SDF-1α, ELC and SLC have been implicated in the physiological recirculation of lymphocytes to lymphoid tissues.[7–12] Because these CKs were not induced with inflammation, it suggested that CKs are functionally segregated.

To determine the contribution of the background non-T-cell innate foreign body CK response, we also assessed CK mRNA produced after embolization of uncoated agarose beads. In general, Ag-free beads elicit minimal transient mononuclear cell inflammation and the CK response was correspondingly blunted. Most transcripts were not significantly induced, reaching only twofold or less than that in normal lungs (data not shown). However, LIX mRNA showed a fivefold induction similar to the type-2 response (as compared to 30-fold for the type-1 response), suggesting that the modest LIX response to SEA beads was essentially Ag-independent. Transient but significant induction was noted on day 1 for MIP-1α, MCP-1, MCP-5, and LARC, with fold increases greater than normal of 4.9, 2.7, 2.7, and 3.5, respectively.

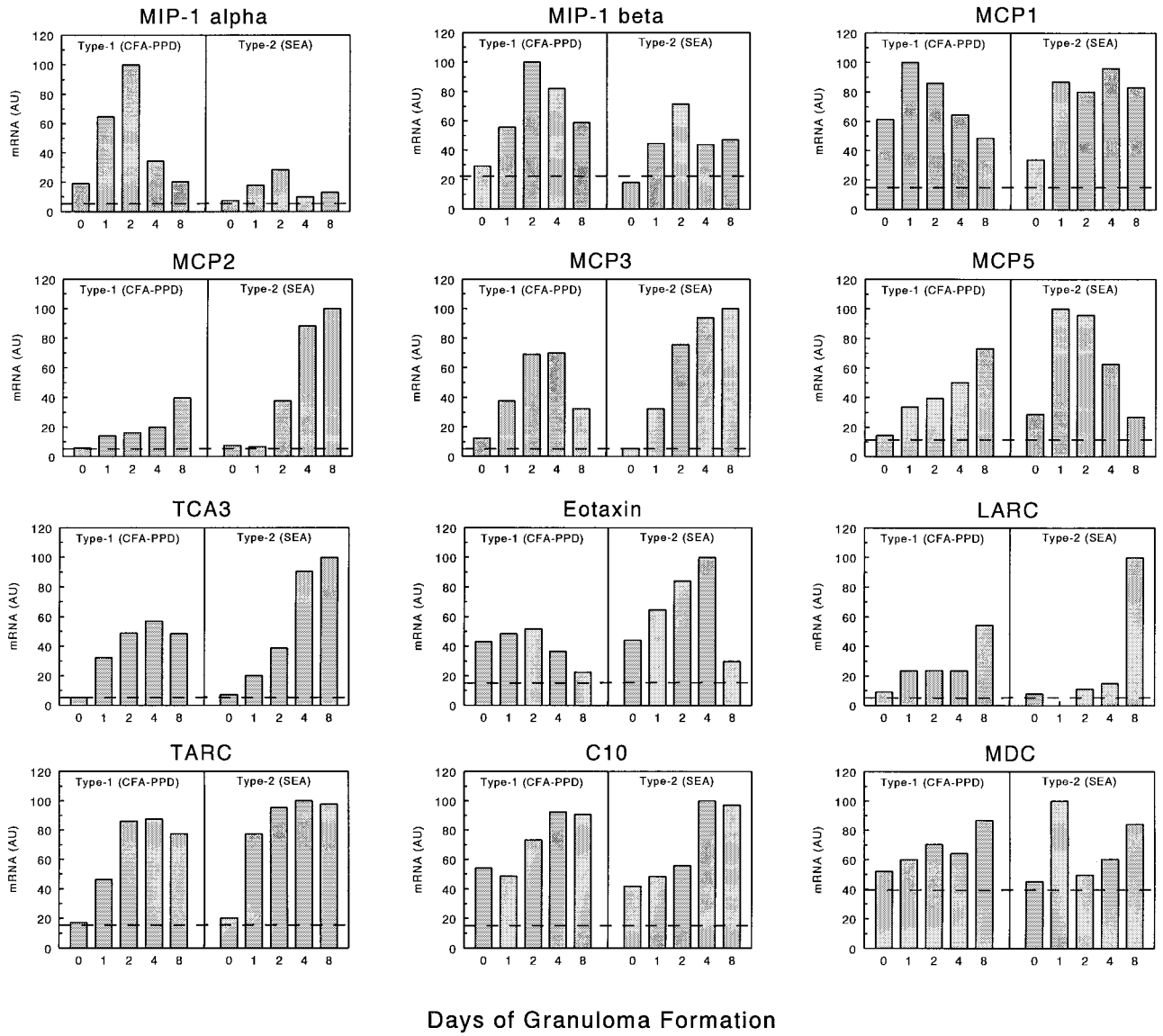

Figure 3. CC chemokine mRNA expression profiles of lungs during type-1 (PPD) and type-2 (SEA) Ag-bead lung granuloma formation. The mRNA expression levels were determined by PCR-ELISA analysis and the results are presented in arbitrary units (AU) as described in Materials and Methods. The profiles are representative of at least three independent experiments. In each experiment mRNA was prepared from three to four mice for each time point. **Dashed lines** indicate levels in normal lung controls.

Although modest compared to the Ag-elicited responses, these inductions suggest participation of CKs in the foreign-body response.

Chemokine Protein Expression Profiles during Type-1 (PPD) and Type-2 (SEA) Pulmonary Granuloma Formation

Because relative CK transcript expression may not necessarily reflect levels of translated protein, we assessed levels of CK in lungs with type-1 and type-2 granulomas by specific protein ELISA. At present, reagents are available to detect only a limited number of murine CKs but where possible such assays were performed. Figure 5 shows levels of CKs detected in lung aqueous extracts during the course of granuloma formation expressed as pg per mg lung protein. In general, CK protein and mRNA expression profiles matched well. As with mRNA, the CXC CKs, IP-10 and MIG dominated in the type-1 response during the early recruitment period. Similarly, MIP-1α and to a lesser extent MIP-1β tended to higher levels in the type-1 response. Likewise reflecting transcript levels, eotaxin dominated in the type-2 response after day 2. As in the transcript analysis, MCP-1/JE and MDC did not display definite polarization and both appeared early in granuloma formation. The KC protein profile differed most from the transcript analysis by showing a clear dominance in the type-1 response. Also, protein analysis showed high levels of C10 that were expressed in ng/mg amounts, which tended to be greater in the type-2 response mainly at the day 8 stage of granuloma formation. This was not apparent from tran-

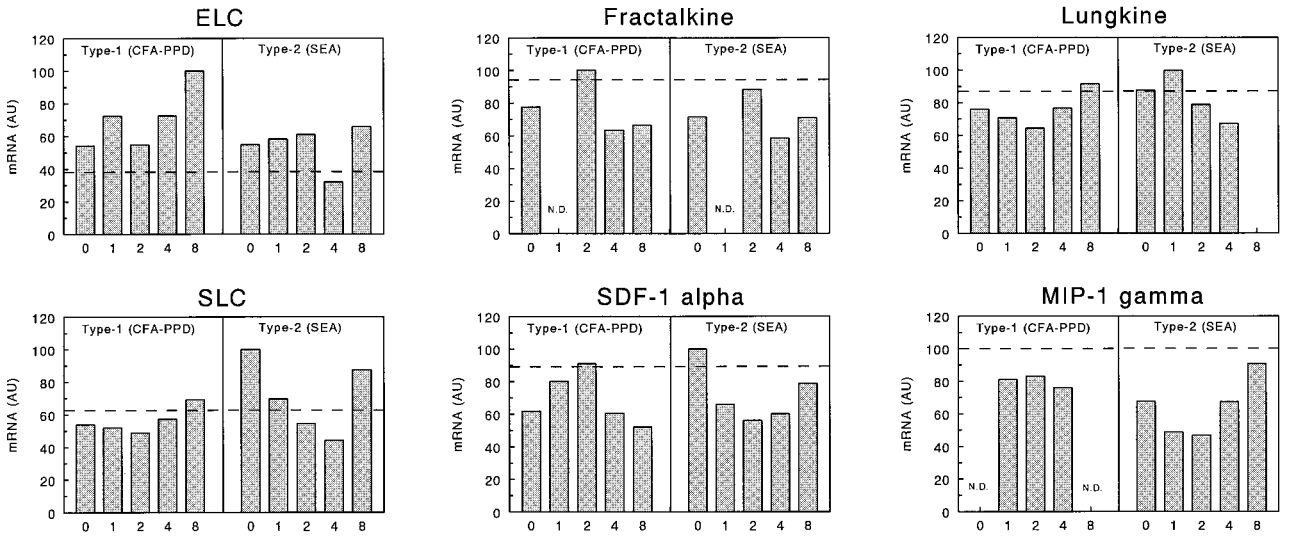

Figure 4. Transcript expression profiles of six constitutively expressed CKs in lungs during type-1 (PPD) and type-2 (SEA) Ag-bead lung granuloma formation. The mRNA expression levels were determined by PCR-ELISA analysis and the results are presented in arbitrary units (AU) as described in Materials and Methods. The profiles are representative of at least three independent experiments. In each experiment mRNA was prepared from three to four mice for each time point. **Dashed lines** indicate levels in normal lung controls. N. D., not done.

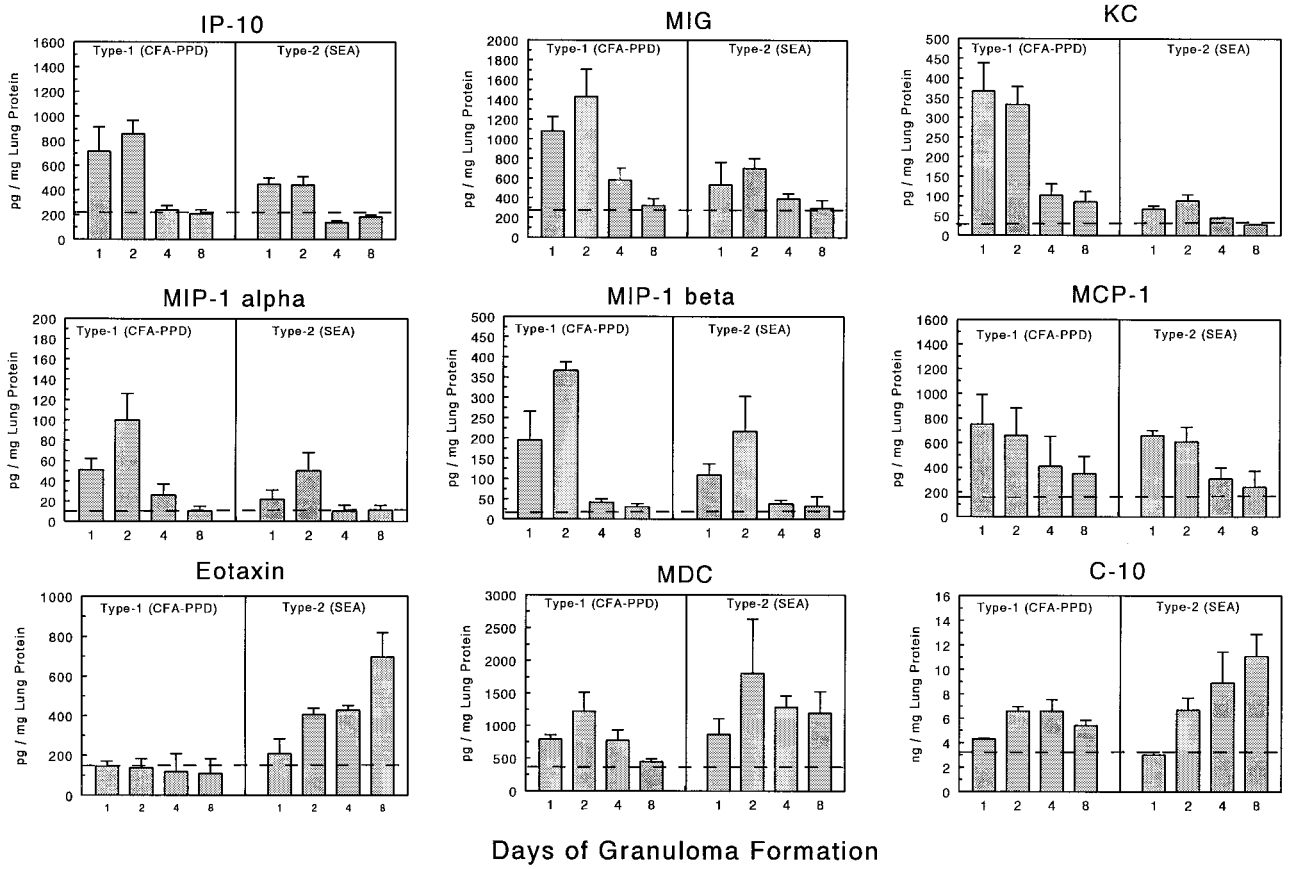

Figure 5. Levels of CKs in lungs during type-1 (PPD) and type-2 (SEA) Ag-bead lung granuloma formation as determined by specific protein immunoassay. Bars are means and SE derived from three separate experiments with a total of 9 to 12 mice per point. All values are normalized to total lung protein. **Dashed lines** indicate levels in normal lung controls.

Table 2. Summary of Chemokine mRNA Expression during Type-1 (PPD) and Type-2 (SEA) Bead Granuloma Formation

Type dominance	Chemokine	Early/late	-Fold increase over normal	Receptors
1	LIX	E	>10	CXCR1,2
1	MIP-2	E	>10	CXCR1,2
1	KC	E	2 to 10	CXCR1,2
1	MIG	E	>10	CXCR3
1	IP-10	E	>10	CXCR3
1	MIP-1α	E	>10	CCR1,5
1	MIP-1β	E	2 to 10	CCR5
1	Lymphotactin	L	2 to 10	XCR1
2	Eotaxin	L	2 to 10	CCR3
2	MCP-2	L	>10	CCR2,3
2	TCA-3	L	>10	CCR8
2	LARC	L	>10	CCR6
2	MCP-3	L	2 to 10	CCR2
1 & 2	MDC	E	2 to 10	CCR4
1 & 2	MCP-1	E	>10	CCR2
1 & 2	MCP-5	E and L	>10	CCR1,2,3
1 & 2	C10	L	2 to 10	CCR?
1 & 2	TARC	E and L	2 to 10	CCR7,8
C	Lungkine	n/a	1 to 2	CXC?
C	SLC	n/a	1 to 2	CXCR3,CCR7
C	ELC	n/a	1 to 2	CCR7
C	Fractalkine	n/a	1 to 2	CX3CR1
C	MIP-1γ	n/a	1 to 2	CCR1,3
C	SDF-1α	n/a	1 to 2	CXCR4

C, Constitutive expression; n/a, does not apply.

script levels. Such discrepancies may be related to local tissue accumulation. Despite this, the findings suggested that semiquantitative mRNA analysis was a reasonably accurate reflection of local CK synthesis. Table 2 summarizes the expression profiles for the 24 CKs analyzed during type-1 and type-2 lung granuloma formation based on transcript and protein analyses.

Cytokine-Mediated Regulation of Chemokine Expression

It is known that Th1-associated cytokines (IFN-γ, TNF-α) promote tissue responses induced by mycobacterial Ags, whereas the Th2-associated cytokines (IL-4, IL-5, and IL-13) mediate those induced by schistosomal egg Ags.[5] Such cytokines may orchestrate inflammatory responses by regulating local CK expression. We previously provided evidence that Th2 cytokine-chemokine networks operate during type-2 lung granuloma formation *in vivo*.[13] In the present study we examined the contribution of IFN-γ in shaping CK expression profiles. A time-course analysis of IFN-γ and IL-5 production by isolated granulomas confirmed the primarily polarized production of IFN-γ by type-1 lesions and indicated that maximum synthesis occurred on days 1 and 2 (Figure 6). This expression correlated well with the observed increase in MIG and IP-10.

Mice were next given intraperitoneal injections of neutralizing anti-murine IFN-γ antibodies just before type-1 or type-2 bead granuloma induction then 2 days later lungs were harvested and CK mRNA levels were measured. Five individual mice were used in this experiment. Three of the mice were treated with neutralizing antibody, and two others were treated with control IgG. Figure 7 shows

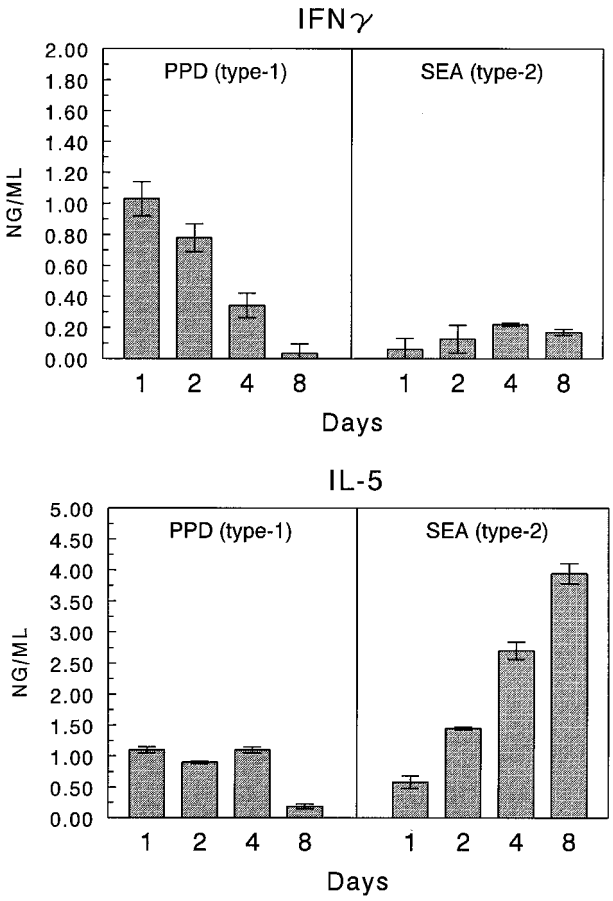

Figure 6. Cytokine production by cultured type-1 (PPD) and type-2 (SEA) Ag-bead lung granulomas. Granulomas were isolated from the lungs (four to five mice per point) and cultured for 48 hours in the presence of either PPD or SEA (5 μg/ml). Supernates were collected and assayed for the indicated cytokines. Bars are means ± SE.

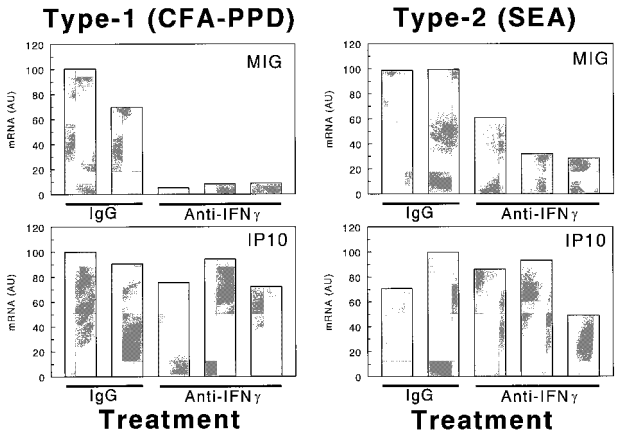

Figure 7. Effect of *in vivo* IFN-γ depletion on MIG and IP-10 transcript levels in lungs with day 2 Ag-bead granulomas. Five individual mice are presented in each type. As indicated, three of the mice are treated with anti-IFN-γ and two with control IgG. The expression levels were determined by PCR-ELISA analysis and the results are presented in arbitrary units (AU) as described in Materials and Methods. Because of the low expression levels in the type-2 lungs, a higher degree of amplification (30 cycles for type 2 *versus* 28 cycles for type 1) was used for detection and revealed that some effect was achieved with IFN-γ neutralization.

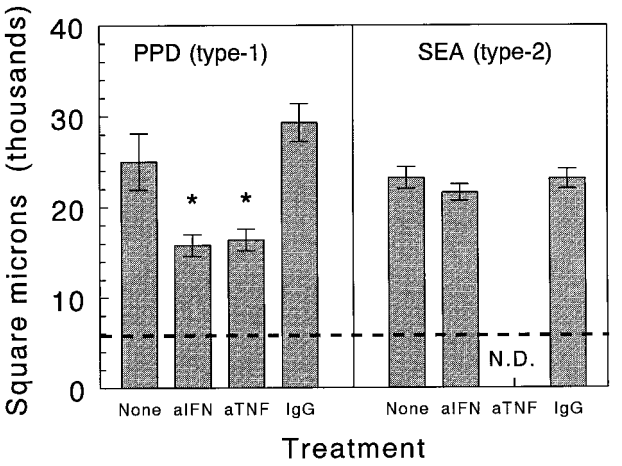

Figure 8. Effect of *in vivo* cytokine depletions on sizes of day 2 Ag-bead lung granulomas. Bars are means ± SE derived from three to four mice. A minimum of 20 granulomas was measured per mouse. **Dashed line** indicates average area occupied by the bead nidus. *, $P < 0.05$. N. D., not done.

the effect on the expression of MIG and IP-10. IFN-γ neutralization profoundly abrogated MIG expression, whereas IP-10 was essentially unchanged. As shown, a similar effect could be demonstrated in the type-2 SEA model by increasing PCR amplification cycle numbers to 30, which allowed detection of the lower levels of these transcripts in this model. Twelve other CKs were also examined after antibody treatment and no significant effect of IFN-γ neutralization could be demonstrated. This data is summarized in Table 3. Thus, IFN-γ seemed to very specifically promote MIG mRNA expression.

Because TNF-α also contributes to type-1 PPD granulomas,[5] TNF-α neutralization was performed in parallel with IFN-γ depletion (Table 3). Unlike the latter, anti-TNF-α reduced a broad range of CKs in the type-1 PPD model. However, the reductions were only partial (50 to 20%) when compared to the controls and fell in the following order MIG > MIP-1α > KC = IP-10 = lymphotactin > MCP-1. As with IFN-γ neutralization certain CKs were unaffected by anti-TNF-α antibodies. Of those examined, these included LIX, MIP-2, LARC, and MCP-5.

Anti-IFN-γ and anti-TNF-α treatments were associated with significant reductions in type-1 PPD granuloma size (Figure 8). Therefore, the CK-abrogating effects may have been in part related to reduced granuloma cellularity. Moreover, the different patterns of abrogation could be related to the different cell populations affected, because as previously reported anti-IFN-γ primarily reduced lymphocytes whereas anti-TNF-α mainly reduced large mononuclear cells.[5]

Table 3. Effect of *in Vivo* Cytokine Depletions on Chemokine mRNA Expression in Lungs with Two-Day, Type-1 (PPD) or Type-2 (SEA) Bead Granulomas

	mRNA expression (arbitrary units)				
	Type 1 (PPD)			Type 2 (SEA)	
Chemokine	IgG	Anti-IFN-γ	Anti-TNF-α	IgG	Anti-IFN-γ
KC	97 ± 3	83 ± 14	64 ± 1*	55 ± 30	66 ± 32
LIX	96 ± 1	98 ± 2	99 ± 1	N.D.	N.D.
MIP-2	65 ± 34	65 ± 15	71 ± 2	N.D.	N.D.
MIG	90 ± 13	14 ± 6*	41 ± 7*	98 ± 2	40 ± 17*
IP-10	95 ± 7	80 ± 12	63 ± 6*	73 ± 18	76 ± 23
Lymphotactin	93 ± 7	86 ± 12	65 ± 1*	62 ± 25	46 ± 11
MIP-1α	95 ± 4	85 ± 13	59 ± 4*	77 ± 21	57 ± 13
LARC	72 ± 19	83 ± 14	67 ± 1	69 ± 13	77 ± 21
MCP-1	86 ± 4	84 ± 14	66 ± 1*	92 ± 6	75 ± 16
MCP-5	70 ± 40	70 ± 10	85 ± 21	78 ± 22	63 ± 34
MCP-2	N.D.	N.D.	N.D.	70 ± 9	68 ± 28
MCP-3	N.D.	N.D.	N.D.	86 ± 8	87 ± 14
Eotaxin	N.D.	N.D.	N.D.	73 ± 25	66 ± 10
TARC	N.D.	N.D.	N.D.	88 ± 8	89 ± 13

Values represent means ± SD derived from analysis of three separate lungs.
*$P < 0.05$.
N.D. = not done.

Discussion

To our knowledge this study represents the first comprehensive analysis comparing CK expression in defined models of type-1 (Th1) and type-2 (Th2) cytokine-mediated inflammatory responses. Although several studies have detected various CKs in human and animal tissue with granulomatous inflammation, the target CKs were limited and experimental conditions were such that temporal dynamics could not be established.[14–19] To date, numerous CKs have been described[1] and the present study was undertaken to determine their expression patterns in defined models of pulmonary granuloma formation. Several important points emerged from this study: 1) granuloma type-specific profiles of CKs were defined, 2) temporal patterns were established indicating coordinated CK expression at key stages of granuloma development revealing CKs with potential pathological relevance, and 3) cytokine-dependent and -independent CK expression was demonstrable. These points are discussed below.

Our study revealed that type-1 (PPD) and type-2 (SEA) bead granuloma responses were associated with distinct CK profiles. Specifically, the CKs fell into four categories: 1) type-1 dominant, 2) type-2 dominant, 3) types 1 and 2 co-dominant, and 4) constitutively expressed with no further induction. These are summarized in Table 2. The type-1-dominant CKs included nearly all of the CXCR1/2, CXCR3, and XCR1 ligands examined. In addition, the CCR1 and CCR5 ligands, MIP-1α and MIP-1β also dominated in the type-1 response. The ELR+, CXCR1/2 ligands are well-described chemotactins for neutrophils and are known to be associated with acute inflammation involving infectious agents[20,21] and tissue injury.[22] Thus, expression during the initial acute phase of granuloma formation might be expected and indeed there was strong induction during the early recruitment period of the type-1 lesion. Furthermore, there was a clear circumstantial association with neutrophil mobilization. At present the origin of the CXCR1/2 ligands during granuloma formation is unknown but mesenchymal cells such as endothelial cells, fibroblasts, and interstitial macrophages are potential sources.

Surprising was the relative paucity of CXCR1/2 ligands in the type-2 response, indicating that the two responses have clearly different initiation phases. Correspondingly, this difference fit well with the lesser degree of neutrophil recruitment in type-2 lesions. One ligand, KC/IL-8, gave some indication of induction by mRNA analysis in the type-2 response, but protein analysis indicated much less than in the type-1 response. This disparity may be related to the neutrophils themselves, which can serve as sources of KC/IL-8 protein[23] and thereby amplify levels in the type-1 response. Another ELR+ ligand, MIP-2, also showed some induction by mRNA analysis in the type-2 response. It is functionally more potent than KC[24] and may be responsible for the small component neutrophil observed in these lesions.

The CXCR3 ligands, IP-10 and MIG, showed the strongest polarization in the type-1 and type 2 responses, with high levels in the former and low levels in the latter by transcript and protein detection. MuMIG and IP-10 are two murine CKs of the non-ELR CXC subfamily that are inducible by the interferons, MuMIG specifically by IFN-γ and IP-10 by IFNs α, β, and γ.[25–27] The enhanced expression of IP-10 and MIG in the type-1 response is in accord with the dominant role of IFN-γ in this response. IP-10 expression is induced by IFN-γ in endothelial cells, monocytes, fibroblasts, keratinocytes,[28,29] astrocytes,[30] and neutrophils.[31] MIG is expressed by IFN-γ-stimulated mononuclear cells, endothelial cells, keratinocytes, and fibroblasts.[26,32] Both MIG and IP-10 are chemotactic for NK cells and activated T lymphocytes *in vitro*, but not resting T cells, B cells, or neutrophils.[32–36] Moreover, IP-10 or MIG expression has been detected in a number of disease conditions with increased expression of IFN-γ such as psoriasis,[18] tuberculoid leprosy,[19] sarcoidosis,[17] tuberculosis,[16] viral meningitis,[37] leishmaniasis,[14] toxoplasmosis,[38] ulcerative colitis,[15] and nephritic nephrosis.[39] Thus, IP-10 and MIG may provide good markers for Th1 or other interferon-dominant responses as suggested by Dixon and colleagues.[40] In this vein, it should be noted that CXCR3 ligands are in themselves potent chemotactins for T lymphocytes, particularly of the Th1 subtype[38,41,42] and in the present study we observed their expression at the time of rapid lymphocyte recruitment, 1 to 2 days.

Two CC CKs, MIP-1α and MIP-1β, were also more prominent in the type-1 response and showed maximum expression on day 2 during the rapid recruitment phase. These CKs are ligands for CCR1 and CCR5 and interestingly have been reported to be associated with type-1 immune responses[43] and demonstrated to be selective attractants for Th1 cells.[44] Our findings lend further *in vivo* support to the association of MIP-1α and MIP-1β to Th1 responses, as well as show a temporal relationship to cell mobilization.

A novel and unexpected finding was the expression pattern of the XCR ligand, lymphotactin, which was more prominent in the type-1 response and showed peak expression on day 4 when the lesions reach the sustenance stage. Lymphotactin is presently the sole representative of the XCR CK class and a well-described chemoattractant for both NK cells and T lymphocytes.[45–47] Enhanced lymphotactin gene expression has been reported in an animal model of glomerulonephritis[48] and is produced by T cells,[49] NK cells,[50] and mast cells.[51] Although lymphotactin exerts a co-stimulatory activity on CD8+ T-cells, it was recently identified as an inhibitor of $CD4^+$ T-cell proliferation and Th1 responses, causing decreased expression of IL-2, IL-2Rα, and IFN-γ but not IL-4 and IL-13.[52] This function may be relevant to our observation that lymphotactin appears as the IFN-γ dominant stage of the Th1 granuloma wanes. Endogenous mediators regulating IFN-γ production in the Th1 granuloma have not previously been identified. Lymphotactin is a good candidate and its later expression suggests that different CKs may usher in various stages of granuloma formation.

With regard to the type-2 response, the CC CKs, eotaxin, MCP-2, MCP-3, TCA-3, and LARC tended to be more dominant than in the type-1 response, but at the transcript level none were totally exclusive. An important

common feature of these CKs is that all showed maximum expression on days 4 or 8, the time when the type-2 lesions become distinguished by their prominent component of eosinophils. It is notable that eotaxin, MCP-2, and MCP-3 are all ligands for CCR3,[1] a receptor that is strongly expressed by eosinophils[53] and is considered important to eosinophil recruitment.[54–56] TCA-3 is a ligand for CCR8, which is also expressed by Th2 cells and may aid in their recruitment. LARC mRNA expression maximized late on day 8, when the granuloma is beginning to resolve. Many leukocytes such as B cells, dendritic cells, $CD4^+$ T cells, and γ-δ T cells[57,58] express the LARC receptor, CCR6. Moreover, there is circumstantial evidence suggesting a role for LARC in inflammation,[57,59] but our findings would indicate that it is likely not involved in the active recruitment stage of granuloma formation. Because the source and target of LARC in granulomatous lungs is as yet unknown, it is difficult to speculate on its function. This question is currently being approached using CCR6 knockout mice.

The third group of CKs (MCP-1, MCP-5, MDC, C10, and TARC) were induced by the inflammatory insult but showed no clear patterns of dominance by transcript analysis. Most were induced by days 1 or 2 then persisted or partially declined by day 8. Protein analyses revealed some trends that were not apparent by mRNA analysis. For example, by protein analysis, both C10 and MDC tended to higher levels in the type-2 response. Accordingly, these CKs are reportedly induced by Th2 cytokines,[60,61] but their presence in the type-1 response would suggest that other factors contribute to their production. The CCR2 ligand, MCP-1/JE, was comparably expressed by protein analysis with peak expression on days 1 and 2. This finding agrees well with our previous demonstration that CCR2-deficient mice show defective macrophage mobilization in both type-1 and type-2 responses precisely at this time.[62,63] The closely homologous MCP-5, another CCR2 ligand, showed peak induction early in the type-2 and delayed induction in the type-1 response. Presently, the significance of these different patterns is unknown, but once reagents become available for muMCP-5 ELISA it may be possible to offer better insights. Unlike MCP-1, there was a sustained induction of TARC mRNA in both models. To date, there is limited data regarding the role of TARC in inflammation. It is a CCR4 ligand that attracts primed $CD4^+$ T cells,[64] in particular IL-4-producing T cells.[65] Interestingly, TARC is up-regulated by both IL-4 and IFN-γ in bronchial epithelial cells, and a maximum production occurred with combination of TNF-α, IL-4, and IFN-γ.[66] Our findings now suggest a common role in granuloma formation. However, further studies will be needed to determine the nature of that participation.

A fourth group of CKs (lungkine, fractalkine, SLC, ELC, MIP-1γ and SDF-α) displayed no or minimal induction after bead challenge. Of these, SLC and ELC are reportedly involved in cellular migration patterns in lymphoid tissues[7–12] and SDF-α in vascular and cerebellar development and hematopoiesis.[67–69] The detected transcripts were possibly derived from endogenous lung-associated lymphoid tissues. Lungkine and MIP-1γ are known to be constitutively expressed by lung tissue[20,70] and their detection was expected. However, our data indicates that no major change is induced by bead granuloma induction. Fractalkine, a mucin-tethered CK, was also unchanged. However, because this CK is expressed by endothelial cells and can potentially act as an adherence molecule,[71] functional participation by preformed molecules remains a possibility.

Another important aspect of our study was the finding of temporal patterns of induced CK expression. This was alluded to above but the point should be emphasized because it reveals that CKs are expressed in a coordinated manner. Serial CK induction has recently been described for two CKs in a mouse model of allergic airway disease.[72] Our study demonstrates this principle in a more comprehensive manner. We showed that some CKs were clearly associated with the early rapid recruitment stage of inflammation whereas others appeared during the sustenance and resolution phases of the response. By relating the temporal expression to histopathological events, hypotheses regarding the source, function, and organization of the various CKs can be designed. For example, very early CKs (eg, MIP-2 and MCP-1) were likely derived from endogenous lung sources, whereas late-early and late CKs (eg, lymphotactin, MCP-3, and LARC) probably arose from recruited cells stimulated by signals provided by the microenvironment. Such a scenario would result in waves of different CKs produced at different stages produced by different cell populations that dictate various inflammatory events from recruitment to resolution.

We have previously demonstrated that CK expression during lung granuloma formation is in part regulated by cytokine stimuli.[6,13] Those studies primarily examined the role of IL-4 and IL-13. In the present study we focused on the role of IFN-γ and TNF-α as upstream regulatory agents. We demonstrated cytokine-dependent and -independent CKs, as well as differences in specificity of cytokine regulation. Of the CKs examined, MIG was highly dependent on IFN-γ, which was predictable based on its known relationship to this cytokine.[32,33] Surprising was the degree of specificity because the other known IFN-γ-induced CK, IP-10, was not dependent. However, it is known that other IFNs can induce IP-10[25] and our finding is consistent with studies of toxoplasma and vaccinia infections, which show differential regulation of MIG and IP-10 with IFN-γ independence of the latter.[73] Our studies showed TNF-α to augment a broader range of CKs but this was an enhancing effect suggesting other underlying inducing factors. Furthermore, some CKs such as LIX and MIP-2 were induced independently of TNF-α as was previously reported in TNF receptor knockout mice stimulated with superantigens.[74] It should be noted that because of the great effort required to monitor numerous CKs in multiple samples we focused analysis on the rapid recruitment period, day 2. Further studies will be needed to determine whether later stage CKs are influenced by cytokine depletions.

In summary, our study indicates that within the redundancy and complexity of CK networks, type-specific and temporal patterns of induction can be defined during

pulmonary granuloma formation. Such profiles will likely be useful in designing CK targeted therapies for chronic inflammatory conditions.

Acknowledgments

We thank Dr. Steven L. Kunkel (University of Michigan) for kindly providing the IFN-γ and TNF-α antisera; and Aron Pollack and Stacey Haller for their expert histological assistance.

References

1. Zlotnik A, Yoshie O: Chemokines: a new classification system and their role in immunity. Immunity 2000, 12:121–127
2. Williams GT, Williams WJ: Granulomatous inflammation—a review. J Clin Pathol 1983, 36:723–733
3. Sheffield EA: The granulomatous inflammatory response. J Pathol 1990, 160:1–2
4. Ben-Baruch A, Michiel DF, Oppenheim JJ: Signals and receptors involved in recruitment of inflammatory cells. J Biol Chem 1995, 270:11703–11706
5. Chensue SW, Warmington KS, Ruth JH, Lincoln P, Kunkel SL: Cytokine function during mycobacterial and schistosomal antigen-induced pulmonary granuloma formation. Local and regional participation of IFN-gamma, IL-10, and TNF. J Immunol 1995, 154:5969–5976
6. Chensue SW, Warmington K, Ruth JH, Lukacs N, Kunkel SL: Mycobacterial and schistosomal antigen-elicited granuloma formation in IFN-gamma and IL-4 knockout mice: analysis of local and regional cytokine and chemokine networks. J Immunol 1997, 159:3565–3573
7. Forster R, Schubel A, Breitfeld D, Kremmer E, Renner-Muller I, Wolf E, Lipp M: CCR7 coordinates the primary immune response by establishing functional microenvironments in secondary lymphoid organs. Cell 1999, 99:23–33
8. Hedrick JA, Zlotnik A: Identification and characterization of a novel beta chemokine containing six conserved cysteines. J Immunol 1997, 159:1589–1593
9. Hromas R, Kim CH, Klemsz M, Krathwohl M, Fife K, Cooper S, Schnizlein-Bick C, Broxmeyer HE: Isolation and characterization of Exodus-2, a novel C-C chemokine with a unique 37-amino acid carboxyl-terminal extension. J Immunol 1997, 159:2554–2558
10. Nagira M, Imai T, Hieshima K, Kusuda J, Ridanpaa M, Takagi S, Nishimura M, Kakizaki M, Nomiyama H, Yoshie O: Molecular cloning of a novel human CC chemokine secondary lymphoid-tissue chemokine that is a potent chemoattractant for lymphocytes and mapped to chromosome 9p13. J Biol Chem 1997, 1951, 272:8–24
11. Randolph DA, Huang G, Carruthers CJ, Bromley LE, Chaplin DD: The role of CCR7 in TH1 and TH2 cell localization and delivery of B cell help in vivo. Science 1999, 286:2159–2162
12. Sallusto F, Lenig D, Forster R, Lipp M, Lanzavecchia A: Two subsets of memory T lymphocytes with distinct homing potentials and effector functions [see comments]. Nature 1999, 401:708–712
13. Ruth JH, Warmington KS, Shang X, Lincoln P, Evanoff H, Kunkel SL, Chensue SW: Interleukin 4 and 13 participation in mycobacterial (type-1) and schistosomal (type-2) antigen-elicited pulmonary granuloma formation: multiparameter analysis of cellular recruitment, chemokine expression and cytokine networks. Cytokine 2000, 12:432–444
14. Cotterell SE, Engwerda CR, Kaye PM: Leishmania donovani infection initiates T cell-independent chemokine responses, which are subsequently amplified in a T cell-dependent manner. Eur J Immunol 1999, 29:203–214
15. Uguccioni M, Gionchetti P, Robbiani DF, Rizzello F, Peruzzo S, Campieri M, Baggiolini M: Increased expression of IP-10, IL-8, MCP-1, and MCP-3 in ulcerative colitis. Am J Pathol 1999, 155:331–336
16. Sauty A, Dziejman M, Taha RA, Iarossi AS, Neote K, Garcia-Zepeda EA, Hamid Q, Luster AD: The T cell-specific CXC chemokines IP-10, Mig, and I-TAC are expressed by activated human bronchial epithelial cells. J Immunol 1999, 162:3549–3558
17. Agostini C, Cassatella M, Zambello R, Trentin L, Gasperini S, Perin A, Piazza F, Siviero M, Facco M, Dziejman M, Chilosi M, Qin S, Luster AD, Semenzato G: Involvement of the IP-10 chemokine in sarcoid granulomatous reactions. J Immunol 1998, 161:6413–6420
18. Gottlieb AB, Luster AD, Posnett DN, Carter DM: Detection of a gamma interferon-induced protein IP-10 in psoriatic plaques. J Exp Med 1988, 168:941–948
19. Kaplan G, Luster AD, Hancock G, Cohn ZA: The expression of a gamma interferon-induced protein (IP-10) in delayed immune responses in human skin. J Exp Med 1987, 166:1098–1108
20. Rossi D, Zlotnik A: The biology of chemokines and their receptors. Annu Rev Immunol 2000, 18:217–242
21. Keane MP, Strieter RM: Chemokine signaling in inflammation. Crit Care Med 2000, 28:N13–N26
22. Lentsch AB, Yoshidome H, Cheadle WG, Miller FN, Edwards MJ: Chemokine involvement in hepatic ischemia/reperfusion injury in mice: roles for macrophage inflammatory protein-2 and KC [corrected and republished article originally printed in Hepatology 1998, 27:507–512]. Hepatology 1998, 27:1172–1177
23. Strieter RM, Kasahara K, Allen RM, Standiford TJ, Rolfe MW, Becker FS, Chensue SW, Kunkel SL: Cytokine-induced neutrophil-derived interleukin-8. Am J Pathol 1992, 141:397–407
24. Lee J, Cacalano G, Camerato T, Toy K, Moore MW, Wood WI: Chemokine binding and activities mediated by the mouse IL-8 receptor. J Immunol 1995, 155:2158–2164
25. Vanguri P, Farber J: Identification of CRG-2. An interferon-inducible mRNA predicted to encode a murine monokine. J Biol Chem 1990, 265:15049–15057
26. Farber JM: A macrophage mRNA selectively induced by gamma-interferon encodes a member of the platelet factor 4 family of cytokines. Proc Natl Acad Sci USA 1990, 87:5238–5242
27. Farber JM: HuMig: a new human member of the chemokine family of cytokines. Biochem Biophys Res Commun 1993, 192:223–230
28. Luster AD, Ravetch JV: Biochemical characterization of a gamma interferon-inducible cytokine (IP-10). J Exp Med 1987, 166:1084–1097
29. Luster AD, Unkeless JC, Ravetch JV: Gamma-interferon transcriptionally regulates an early-response gene containing homology to platelet proteins. Nature 1985, 315:672–676
30. Ransohoff RM, Hamilton TA, Tani M, Stoler MH, Shick HE, Major JA, Estes ML, Thomas DM, Tuohy VK: Astrocyte expression of mRNA encoding cytokines IP-10 and JE/MCP-1 in experimental autoimmune encephalomyelitis. FASEB J 1993, 7:592–600
31. Cassatella MA, Gasperini S, Calzetti F, Bertagnin A, Luster AD, McDonald PP: Regulated production of the interferon-gamma-inducible protein-10 (IP-10) chemokine by human neutrophils. Eur J Immunol 1997, 27:111–115
32. Farber JM: Mig and IP-10: CXC chemokines that target lymphocytes. J Leukoc Biol 1997, 61:246–257
33. Liao F, Rabin RL, Yannelli JR, Koniaris LG, Vanguri P, Farber JM: Human Mig chemokine: biochemical and functional characterization. J Exp Med 1995, 182:1301–1314
34. Maghazachi AA, Skalhegg BS, Rolstad B, Al-Aoukaty A: Interferon-inducible protein-10 and lymphotactin induce the chemotaxis and mobilization of intracellular calcium in natural killer cells through pertussis toxin-sensitive and -insensitive heterotrimeric G-proteins. FASEB J 1997, 11:765–774
35. Taub DD, Lloyd AR, Conlon K, Wang JM, Ortaldo JR, Harada A, Matsushima K, Kelvin DJ, Oppenheim JJ: Recombinant human interferon-inducible protein 10 is a chemoattractant for human monocytes and T lymphocytes and promotes T cell adhesion to endothelial cells. J Exp Med 1993, 177:1809–1814
36. Taub DD, Sayers TJ, Carter CR, Ortaldo JR: Alpha and beta chemokines induce NK cell migration and enhance NK-mediated cytolysis. J Immunol 1995, 155:3877–3888
37. Lahrtz F, Piali L, Nadal D, Pfister HW, Spanaus KS, Baggiolini M, Fontana A: Chemotactic activity on mononuclear cells in the cerebrospinal fluid of patients with viral meningitis is mediated by interferon-gamma inducible protein-10 and monocyte chemotactic protein-1. Eur J Immunol 1997, 27:2484–2489
38. Khan IA, MacLean JA, Lee FS, Casciotti L, DeHaan E, Schwartzman

JD, Luster AD: IP-10 is critical for effector T cell trafficking and host survival in Toxoplasma gondii infection. Immunity 2000, 12:483–494
39. Gomez-Chiarri M, Ortiz A, Gonzalez-Cuadrado S, Seron D, Emancipator SN, Hamilton TA, Barat A, Plaza JJ, Gonzalez E, Egido J: Interferon-inducible protein-10 is highly expressed in rats with experimental nephrosis. Am J Pathol 1996, 148:301–311
40. Dixon AE, Mandac JB, Madtes DK, Martin PJ, Clark JG: Chemokine expression in Th1 cell-induced lung injury: prominence of IFN-gamma-inducible chemokines. Am J Physiol 2000, 279:592–599
41. Liu MT, Chen BP, Oertel P, Buchmeier MJ, Armstrong D, Hamilton TA, Lane TE: Cutting Edge: the T cell chemoattractant IFN-inducible protein 10 is essential in host defense against viral-induced neurologic disease. J Immunol 2000, 165:2327–2330
42. Tannenbaum CS, Tubbs R, Armstrong D, Finke JH, Bukowski RM, Hamilton TA: The CXC chemokines IP-10 and Mig are necessary for IL-12-mediated regression of the mouse RENCA tumor. J Immunol 1998, 161:927–932
43. Schrum S, Probst P, Fleischer B, Zipfel PF: Synthesis of the CC-chemokines MIP-1alpha, MIP-1beta, and RANTES is associated with a type 1 immune response. J Immunol 1996, 157:3598–3604
44. Siveke JT, Hamann A: T helper 1 and T helper 2 cells respond differentially to chemokines. J Immunol 1998, 160:550–554
45. Hedrick JA, Saylor V, Figueroa D, Mizoue L, Xu Y, Menon S, Abrams J, Handel T, Zlotnik A: Lymphotactin is produced by NK cells and attracts both NK cells and T cells in vivo. J Immunol 1997, 158:1533–1540
46. Giancarlo B, Silvano S, Albert Z, Mantovani A, Allavena P: Migratory response of human natural killer cells to lymphotactin. Eur J Immunol 1996, 26:3238–3241
47. Wang JD, Nonomura N, Takahara S, Li BS, Azuma H, Ichimaru N, Kokado Y, Matsumiya K, Miki T, Suzuki S, Okuyama A: Lymphotactin: a key regulator of lymphocyte trafficking during acute graft rejection. Immunology 1998, 95:56–61
48. Natori Y, Ou ZL, Yamamoto-Shuda Y: Expression of lymphotactin mRNA in experimental crescentic glomerulonephritis. Clin Exp Immunol 1998, 113:265–268
49. Kelner GS, Kennedy J, Bacon KB, Kleyensteuber S, Largaespada DA, Jenkins NA, Copeland NG, Bazan JF, Moore KW, Schall TJ, Zlotnik A: Lymphotactin: a cytokine that represents a new class of chemokine. Science 1994, 266:1395–1399
50. Hennemann B, Tam YK, Tonn T, Klingemann HG: Expression of SCM-1alpha/lymphotactin and SCM-1beta in natural killer cells is upregulated by IL-2 and IL-12. DNA Cell Biol 1999, 18:565–571
51. Rumsaeng V, Vliagoftis H, Oh CK, Metcalfe DD: Lymphotactin gene expression in mast cells following Fc(epsilon) receptor I aggregation: modulation by TGF-beta, IL-4, dexamethasone, and cyclosporin A. J Immunol 1997, 158:1353–1360
52. Cerdan C, Serfling E, Olive D: The C-class chemokine, lymphotactin, impairs the induction of Th1-type lymphokines in human CD4(+) T cells. Blood 2000, 96:420–428
53. Ponath PD, Qin S, Post TW, Wang J, Wu L, Gerard NP, Newman W, Gerard C, Mackay CR: Molecular cloning and characterization of a human eotaxin receptor expressed selectively on eosinophils [see Comments]. J Exp Med 1996, 183:2437–2448
54. Gerber BO, Zanni MP, Uguccioni M, Loetscher M, Mackay CR, Pichler WJ, Yawalkar N, Baggiolini M, Moser B: Functional expression of the eotaxin receptor CCR3 in T lymphocytes co-localizing with eosinophils. Curr Biol 1997, 7:836–843
55. Sabroe I, Conroy DM, Gerard NP, Li Y, Collins PD, Post TW, Jose PJ, Williams TJ, Gerard CJ, Ponath PD: Cloning and characterization of the guinea pig eosinophil eotaxin receptor, C-C chemokine receptor-3: blockade using a monoclonal antibody in vivo. J Immunol 1998, 161:6139–6147
56. Teixeira MM, Wells TN, Lukacs NW, Proudfoot AE, Kunkel SL, Williams TJ, Hellewell PG: Chemokine-induced eosinophil recruitment. Evidence of a role for endogenous eotaxin in an in vivo allergy model in mouse skin. J Clin Invest 1997, 100:1657–1666
57. Tanaka Y, Imai T, Baba M, Ishikawa I, Uehira M, Nomiyama H, Yoshie O: Selective expression of liver and activation-regulated chemokine (LARC) in intestinal epithelium in mice and humans. Eur J Immunol 1999, 29:633–642
58. Varona R, Zaballos A, Gutierrez J, Martin P, Roncal F, Albar JP, Ardavin C, Marquez G: Molecular cloning, functional characterization and mRNA expression analysis of the murine chemokine receptor CCR6 and its specific ligand MIP-3alpha. FEBS Lett 1998, 440:188–194
59. Utans-Schneitz U, Lorez H, Klinkert WE, da Silva J, Lesslauer W: A novel rat CC chemokine, identified by targeted differential display, is upregulated in brain inflammation [published erratum appears in J Neuroimmunol 1999, Feb 1;94(1–2):222]. J Neuroimmunol 1998, 92:179–190
60. Andrew DP, Chang MS, McNinch J, Wathen ST, Rihanek M, Tseng J, Spellberg JP, Elias III CG: STCP-1 (MDC) CC chemokine acts specifically on chronically activated Th2 lymphocytes and is produced by monocytes on stimulation with Th2 cytokines IL-4 and IL-13. J Immunol 1998, 161:5027–5038
61. Orlofsky A, Wu Y, Prystowsky MB: Divergent regulation of the murine CC chemokine C10 by Th(1) and Th(2) cytokines. Cytokine 2000, 12:220–228
62. Boring L, Gosling J, Chensue SW, Kunkel SL, Farese Jr RV, Broxmeyer HE, Charo IF: Impaired monocyte migration and reduced type 1 (Th1) cytokine responses in C-C chemokine receptor 2 knockout mice. J Clin Invest 1997, 100:2552–2561
63. Warmington KS, Boring L, Ruth JH, Sonstein J, Hogaboam CM, Curtis JL, Kunkel SL, Charo IR, Chensue SW: Effect of C-C chemokine receptor 2 (CCR2) knockout on type-2 (schistosomal antigen-elicited) pulmonary granuloma formation: analysis of cellular recruitment and cytokine responses. Am J Pathol 1999, 154:1407–1416
64. Lieberam I, Forster I: The murine beta-chemokine TARC is expressed by subsets of dendritic cells and attracts primed CD4+ T cells. Eur J Immunol 1999, 29:2684–2694
65. Yoneyama H, Harada A, Imai T, Baba M, Yoshie O, Zhang Y, Higashi H, Murai M, Asakura H, Matsushima K: Pivotal role of TARC, a CC chemokine, in bacteria-induced fulminant hepatic failure in mice. J Clin Invest 1998, 102:1933–1941
66. Sekiya T, Miyamasu M, Imanishi M, Yamada H, Nakajima T, Yamaguchi M, Fujisawa T, Pawankar R, Sano Y, Ohta K, Ishii A, Morita Y, Yamamoto K, Matsushima K, Yoshieo, Hirai K: Inducible expression of a Th2-type CC chemokine thymus- and activation-regulated chemokine by human bronchial epithelial cells. J Immunol 2000, 165:2205–2213
67. Nagasawa T, Hirota S, Tachibana K, Takakura N, Nishikawa S, Kitamura Y, Yoshida N, Kikutani H, Kishimoto T: Defects of B-cell lymphopoiesis and bone-marrow myelopoiesis in mice lacking the CXC chemokine PBSF/SDF-1. Nature 1996, 382:635–638
68. Zou YR, Kottmann AH, Kuroda M, Taniuchi I, Littman DR: Function of the chemokine receptor CXCR4 in haematopoiesis and in cerebellar development [see Comments]. Nature 1998, 393:595–599
69. Tachibana K, Hirota S, Iizasa H, Yoshida H, Kawabata K, Kataoka Y, Kitamura Y, Matsushima K, Yoshida N, Nishikawa S, Kishimoto T, Nagasawa T: The chemokine receptor CXCR4 is essential for vascularization of the gastrointestinal tract [see Comments]. Nature 1998, 393:591–594
70. Poltorak AN, Bazzoni F, Smirnova II, Alejos E, Thompson P, Luheshi G, Rothwell N, Beutler B: MIP-1 gamma: molecular cloning, expression, and biological activities of a novel CC chemokine that is constitutively secreted in vivo. J Inflammation 1995, 45:207–219
71. Fong AM, Robinson LA, Steeber DA, Tedder TF, Yoshie O, Imai T, Patel DD: Fractalkine and CX3CR1 mediate a novel mechanism of leukocyte capture, firm adhesion, and activation under physiologic flow. J Exp Med 1998, 188:1413–1419
72. Lloyd CM, Delaney T, Nguyen T, Tian J, Martinez AC, Coyle AJ, Gutierrez-Ramos JC: CC chemokine receptor (CCR)3/eotaxin is followed by CCR4/monocyte-derived chemokine in mediating pulmonary T helper lymphocyte type 2 recruitment after serial antigen challenge in vivo. J Exp Med 2000, 191:265–274
73. Amichay D, Gazzinelli RT, Karupiah G, Moench TR, Sher A, Farber JM: Genes for chemokines MuMig and Crg-2 are induced in protozoan and viral infections in response to IFN-gamma with patterns of tissue expression that suggest nonredundant roles in vivo. J Immunol 1996, 157:4511–4520
74. Neumann B, Emmanuilidis K, Stadler M, Holzmann B: Distinct functions of interferon-gamma for chemokine expression in models of acute lung inflammation. Immunology 1998, 95:512–521